The shifting of secondary inorganic aerosols formation mechanism during haze aggravation: The decisive role of aerosol liquid water

Fei Xie[1, 2], Yue Su[1, 3], Yongli Tian[2], Yanju Shi[2], Xingjun Zhou[2], Peng Wang[2], Ruihong Yu[1], Wei Wang[1], Jiang He[1, 3], Jinyuan Xin[4, *], Changwei Lü[1, 3, *]

[1] *School of Ecology and Environment, Inner Mongolia University, 010021, Hohhot, China*

[2] *Inner Mongolia Environmental Monitoring Center, 010011, Hohhot, China*

[3] *Institute of Environmental Geology, Inner Mongolia University, 010021, Hohhot, China*

[4]*State Key Laboratory of Atmospheric Boundary Layer Physics and Atmospheric Chemistry (LAPC), Institute of Atmospheric Physics, Chinese Academy of Sciences, Beijing 100029, China*

Abstract

Although many considerable efforts have been done to reveal the driving factors on haze aggravation, however, the roles of aerosol liquid water (ALW) in SIAs formation were mainly focused on the condition of aerosol liquid water content (ALWC)<100 $\mu g/m^3$. Based on the in-situ high-resolution field observation, this work studied the decisive roles and the shifting of secondary inorganic aerosols formation mechanism during haze aggravation, revealing the different roles of ALWC in a broader scale (~ 500 $\mu g/m^3$) in nitrate and sulfate formation induced by aqueous chemistry in ammonia-rich atmosphere. The results showed that chemical domains of perturbation gas limiting the generation of secondary particulate matters presented obvious shifts from HNO_3 sensitive to HNO_3 and NH_3 co-sensitive regime with the haze aggravation, indicating the powerful driving effects of ammonia in ammonia-rich atmosphere. When ALWC<75 $\mu g/m^3$, the sulfate generation was preferentially triggered by the high ammonia utilization, then accelerated by nitrogen oxide oxidation from Clean to Moderate pollution stages, characterizing as nitrogen oxidation ratio (NOR)<0.3, sulfur oxidation ratio (SOR)<0.4, ammonia transition ratio (NTR)<0.7 and the moral ratio of NO_3^-/SO_4^{2-}=2:1. While ALWC>75 $\mu g/m^3$, aqueous-phase chemistry reaction of SO_2 and NH_3 in ALW became the prerequisite for SIAs formation driven by Henry's law in the ammonia-rich atmosphere during Heavy and Serious stages, characterizing as high SOR (0.5-0.9), NOR (0.3-0.5), NTR (>0.7) and the moral ratio of NO_3^-/SO_4^{2-}=1:1. A positive feedback of sulfate on nitrate production was also observed in this work due to the shift of ammonia partition induced by the ALWC variation during haze aggravation. It implies the target controlling of haze should not simply focus on SO_2 and NO_2, more attention should be paid on gaseous precursors (e.g., SO_2, NO_2, NH_3) and aerosol chemical constitution during different haze stages.

Keywords: Mechanism shifting, Aerosol liquid water, Secondary inorganic aerosols, Haze aggravation, In-situ observation

---

* Corresponding author, Email: xjy@mail.iap.ac.cn; lcw2008@imu.edu.cn

1 Introduction

Fine particulate matter (PM2.5) presented close link with several environmental issues, such as visibility reduction and climate change (Zhang et al., 2015; Shang et al., 2020; Wang et al., 2020; Wang et al., 2016; Nozière et al., 2010). Epidemiological studies have stated the association of PMs with various public health, even adverse birth outcomes (Gwynn et al., 2000; Lavigne et al., 2016; Zhao et al., 2020). As the most abundant secondary inorganic aerosols (SIAs) in PM2.5 during Chinese winter haze episodes (Fu and Chen, 2017; Liu et al., 2019), the formations of sulfate and nitrate play the key roles during haze aggravation, as well as the impacting factors of the oxidants in gas and aqueous phases, the characteristics of pre-existing aerosols/fog/cloud, and meteorological conditions. Recently, aerosol liquid water content (ALWC) was reported associating with the SIAs formation, especially sulfates and nitrates, during the haze periods (Wu et al., 2018; Zheng et al., 2015a; Wang et al., 2016; Cheng et al., 2016; Carlton and Turpin, 2013; Nguyen et al., 2014; Xue et al., 2014; Tan et al., 2017; Liu et al., 2017b). Atmospheric aerosol liquid water (ALW), which determined by ambient relative humidity (RH), has been proposed as a container since it could provide the reaction medium for the multiphase chemistry during the haze process (Ansari and Pandis, 2000; Shiraiwa et al., 2012; Davies and Wilson, 2015). The roles of ALWC on the generations of particulate sulfate generations (Wang et al., 2016; Cheng et al., 2016) and global secondary organic aerosols (Hodas et al., 2014; Mcneill, 2015; Wong et al., 2015) were reported. Thus, fully understanding ALW and its roles during haze aggravation is fundamentally important on atmospheric physicochemical processes, especially the liquid chemical transformation of SO_2 and NO_x in ALW.

Ammonia is the most important alkaline gas, neutralizing with acidic species to form ammonium salts. Due to little attention has been paid to NH_3 emissions by Chinese government, atmospheric NH_3 experienced a significant increasing trend (Ge et al., 2019; Tan et al., 2017). Although the increase in atmospheric NH_3 is beneficial to reduce atmospheric acidity (Liu et al., 2019), its chemical behavior on regional haze formation is still debating. Cheng et al. (2016) indicated that the fast transform of gaseous SO_2 to particle sulfate under polluted conditions is attributed to the neutralization of NH_3, which raises particle pH and thereby facilitated the aqueous oxidation of S (VI) by NO_2. Fang et al. (2017) stated that NH_3 partition significantly modified aerosol pH and thereby adjusting the partition of SO_2 and NO_2. Although the role of NH_3 has been identified from a theoretical perspective, the lack of NH_3 emission control sets barriers for more effective reduction of PM2.5. Therefore, it is urgent to fully understand the reactive gases behavior and the chemical mechanism of SIAs formation during different

pollution stages, which will be helpful to propose reasonable strategies for each stage.

So far, the SIAs formation has been extensively studied during short-term, continuous, or persistent haze episodes, proposing several heterogeneous and homogeneous oxidation pathways on sulfate and nitrate formation (Guo et al., 2014; Guo et al., 2017; Zheng et al., 2015b; Huang et al., 2014; Liu et al., 2021; Yao et al., 2020; Zhou et al., 2018; Liu et al., 2019). In ammonia-rich atmosphere, NH_3 partition significantly modified aerosol pH, adjusted the partition of SO_2 and NO_2 (Fang et al., 2017) and promotes the aqueous oxidation of S (VI) by NO_2 (Wang et al., 2016; Cheng et al., 2016). Although many considerable efforts have been done to reveal the driving factors on haze aggravation, however, the roles of ALW in SIAs formation were mainly focused on the condition of ALWC<100 $\mu g/m^3$ (Nenes et al., 2020; Wu et al., 2018; Bian et al., 2014; Jin et al., 2020). Therefore, the roles of ALWC in a broader scale and the mechanism shifting of secondary inorganic aerosols formation during haze aggravation in ammonia-rich atmosphere need to be understood in depth. Based on a continuous observation with 1-hour resolution from December 2019 to January 2020, this work discussed the shift of dominant mechanism with ALWC variation during the time window of haze aggravation processes, which will be helpful to propose more effective $PM_{2.5}$ control strategies for each pollution stage.

2 Sampling and Experiment Methods

2.1 Description of Sampling Site

Hohhot, the capital city of Inner Mongolia Autonomous Region, is the central city of Hohhot-Baotou-Ordos group, as well as an important northern China city with a population of more than 3.126 million and an area of 17224 km^2 (Fig. 1). This region is featured as continental climate with marked seasonality changes, which characterized as long-lasting cold humid winter and short-time other seasons. Thereby, to survive the cold season, approximately half year of coal-fired heating events (Oct. 15-the following Apr. 15) were introduced, which emitting gaseous pollutants as well as PMs around-the-clock. The main industries include thermal power plants, coal-energy based biochemical industry, dairy industry and petrochemical industry, etc., which also emit atmospheric pollutants ceaselessly. Thus, high concentrations of PMs pollution cases dominated the major contamination cases during winter season (data obtained from Department of Ecology and Environment of Inner Mongolia Autonomous Region, http://sthjt.nmg.gov.cn/) and gradually emerging as the limiting factor on regional ambient air quality and human health.

In this study, the observation was conducted at the Inner Mongolia Environmental

Monitoring Center (40°49′22″N, 111°45′2″E) on a top of a sixteen-story building (~40m above the ground level) located at the eastern part of the downtown near the People's Government of Inner Mongolia Autonomous Region near the 2nd ring road from December 1, 2019 to January 31, 2020. Residential and administrative regions were characterized as the major functional domain near the sampling site, with no direct industrial regions nearby.

Fig. 1 Map of sampling sites and coal-fired enterprises
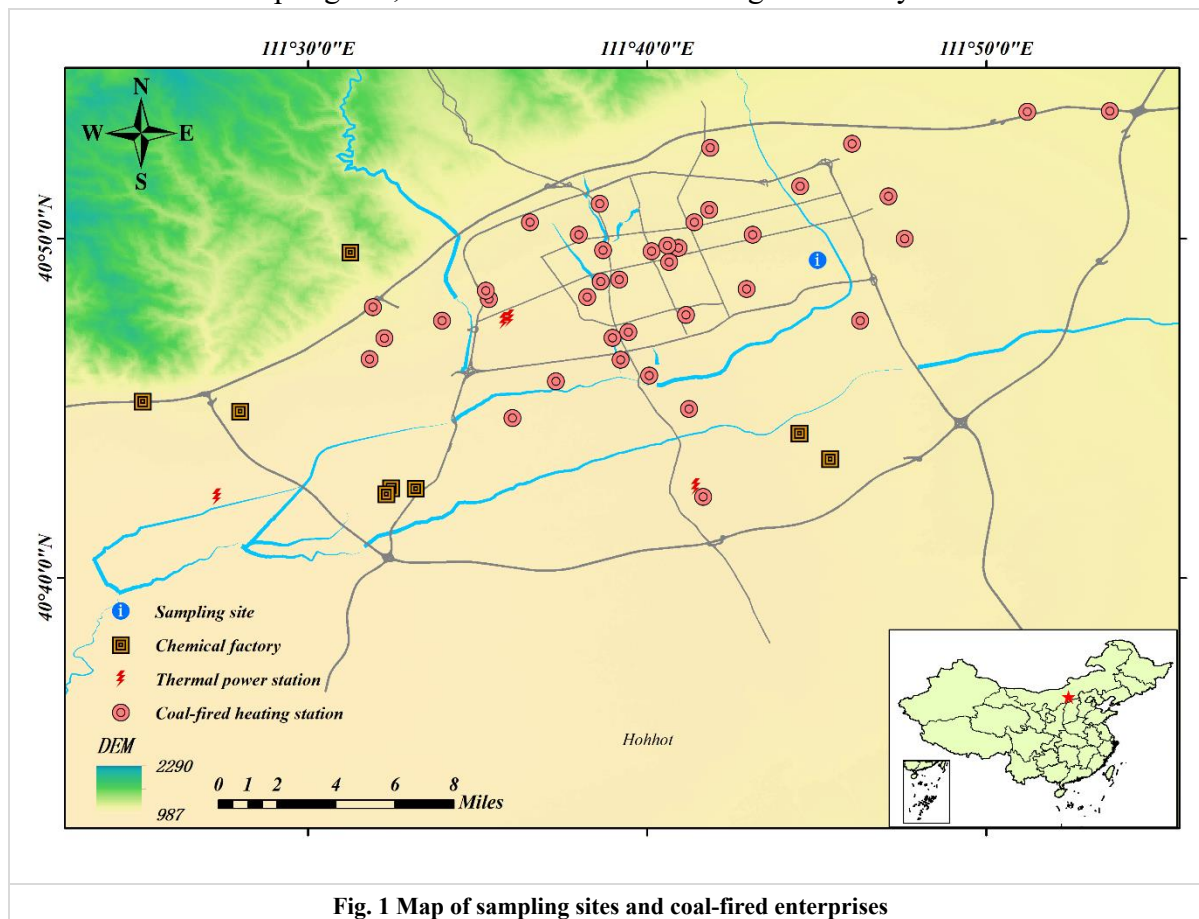
2.2 Data acquisition and analysis methods

2.2.1 Data acquisition

On-line ion-chromatograph instrument (MARGA ADI 2080, Metrohm Applikon, Switzerland) was employed to simultaneously determine the water-soluble inorganic ions (Na^+, NH_4^+, Mg^{2+}, Ca^{2+}, K^+, Cl^-, F^-, SO_4^{2-}, NO_3^-) in $PM_{2.5}$ and corresponding trace gases (SO_2, HNO_2, HNO_3, HCl, NH_3).This instrument has been widely used in previous work (Rumsey et al., 2014; Nie et al., 2015; Huang et al., 2020) and the details were listed in Supplement (S1.1). Correspondingly, gaseous pollutants (e.g., NO_x, CO, PM_1, $PM_{2.5}$, PM_{10}) and meteorological datasets (e.g., wind speed, wind direction, RH, temperature, etc.), as well as the adopted models could be found in our previous work (Xie et al., 2021). In addition, peroxyacetyl nitrates (PANs), nitrous oxide (N_2O) and solar spectrophotometry were measured by PANs-100 (Focused Photonics Inc.),

120 N$_2$O Monitor (LSE, Monitors) and CE-318T (CIMEL), respectively.

121

122 **2.2.2 Analysis methods**

123 Generally, sulfur oxidation ratio (SOR) and nitrogen oxidation ratio (NOR) were calculated as

124 follows, which were used to indicate the contribution of secondary transformation during the

125 haze events (Song et al., 2007; Zhou et al., 2018).

126
$$SOR = \frac{n(SO_4^{2-})}{n(SO_2) + n(SO_4^{2-})}$$

127
$$NOR = \frac{n(HNO_3) + n(NO_3^-)}{n(NO_2) + n(HNO_3) + n(NO_3^-)}$$

128 Meanwhile, as an indicator of ammonia conversion efficient, ammonia transition ratio

129 (NTR), was calculated as the following equation (All units were μg/m^3).

130
$$NTR = \frac{NH_4^+/18}{NH_4^+/18 + NH_3/22.4}$$

131 In addition, as the fractions of ammonia, nitrate and sulfate in deliquesced aerosol, ε

132 (NO$_3$$^-$), ε(NH$_4$$^+$) and ε(SO$_4$$^{2-}$) were expressed as follows.

133
$$\varepsilon(NO_3^-) = \frac{n(NO_3^-)}{n(HNO_3) + n(NO_3^-)}$$

134
$$\varepsilon(NH_4^+) = \frac{n(NH_4^+)}{n(NH_3) + n(NH_4^+)}$$

135
$$\varepsilon(SO_4^{2-}) = \frac{n(SO_4^{2-})}{n(SO_2) + n(SO_4^{2-})}$$

136 **2.2.3 Aerosol pH**

137 In this work, a widely used thermodynamic model, ISORROPIA-II (Song et al., 2018; Gao et

138 al., 2020), was employed to establish aerosol acidity. Including the concentrations of WSIs in

139 PM$_{2.5}$ and gaseous pollutions (e.g., NH$_3$, HCl), the simultaneously measured temperature and

140 RH data were imported into its Na$^+$-K$^+$-Ca^{2+}-Mg^{2+}-NH$_4$$^+$-SO$_4$$^{2-}$-NO$_3$$^-$-Cl$^-$-H$_2$O aerosol system.

141 According to previous study (Song et al., 2018) and our data profiles, "Forward Mode" and

142 "Metastable State" were selected in the model of ISORROPIA-II to calculate aerosol acidity

143 (H$_{air}$$^+$, H$^+$ loading per volume air (μg/m^3)) and aerosol liquid water content (ALWC). Then the

144 aerosol pH was calculated by the following equation.

145
$$pH = -\log_{10}\frac{1000H_{air}^+}{ALWC}$$

146 The concentrations of NH$_3$, NH$_4$$^+$, NO$_3$$^-$ and SO$_4$$^{2-}$ modeled by this model significantly

147 correlated with their measured values with correlation coefficients of 0.971-0.999, indicating

148 the accuracy and acceptability of the model in this work (Fig. S1).

149 ***2.2.4 Heterogeneous sulfate production***

150 Due to the necessity of precise SO_4^{2-} generation, heterogeneous sulfate production (P_{het}) was

151 parameterized and calculated according to the following equation(Jacob, 2000; Zheng et al.,

152 2015a),

$$P_{het} = \frac{3600sh^{-1} \times 96gmol^{-1} \times P}{R \times T} \left(\frac{R_p}{D_g} + \frac{4}{\upsilon\gamma} \right)^{-1} S_p[SO_2(g)]$$

154 Where P_{het} was presented in $\mu g \cdot m^{-3} \cdot h^{-1}$, $3600sh^{-1}$ is time conversion factor, 96 g/mol is the

155 molar mass of SO_4^{2-}, P is atmospheric pressure in kPa, R is the gas constant with the value of

156 8.31 $Pa \cdot m^3 \cdot mol^{-1} \cdot K^{-1}\cdot$, T is the temperature with the unit of K, R_p represented the radius of

157 aerosol particles (m), D_g is the SO_2 molecular diffusion coefficient and υ is the mean molecular

158 speed of SO_2 with the typical tropospheric value of $2\times10^{-5} m^2 \cdot s^{-1}$ and 300 $m \cdot s^{-1}$, respectively. γ

159 is the uptake coefficient of SO_2 on aerosols, S_p is the aerosol surface area per unit volume of

160 air ($m^2 \cdot m^{-3}$) (Jacob, 2000). $PM_{2.5}$ mass concentrations ($\mu g \cdot m^{-3}$) and mean radius (m) during

161 campaign were roughly calculated utilizing the following empirical formula published by Guo

162 et al. (2014):

$$R_p = \left(0.254 \times C_{(PM_{2.5})} + 10.259 \right) \times 10^{-9}$$

164 mean density of particles ρ was calculated and showed as 1.5×10^6 $g \cdot m^{-3}$ using the volume

165 and surface area formulas of a sphere (Guo et al., 2014). S_p was estimated from the following

166 formula:

$$S_p = \frac{C_{(PM_{2.5})} \times 10^{-6} g \cdot \mu g^{-1}}{4/3 \cdot \pi R_p^3 \cdot \rho} \cdot 4\pi R_p^2$$

168 relative humidity-dependent γ were derived according to Zheng et al. (2015a) during the

169 campaign in this work and showed as the following formular:

$$\gamma = \begin{cases} 2 \times 10^{-5}, & \Psi \le 50\%, \\ 2 \times 10^{-5} + \dfrac{5 \times 10^{-5} - 2 \times 10^{-5}}{100 - 50\%} \times (\Psi - 50\%), & 50\% \le \Psi \le 100\% \end{cases}$$

171 where ψ referred to RH with the unit of %.

3 Results and Discussion

173 Based on National Ambient Air Quality Standards of China (HJ633-2012)

174 (https://www.mee.gov.cn/ywgz/fgbz/bz/bzwb/jcffbz/201203/t20120302_224166.shtml), air

175 quality index (AQI) was introduced in this work to classify pollution levels (Wang et al., 2015;

Kanchan et al., 2015; Xu et al., 2017) and discuss the characteristics of atmospheric pollutants. Briefly, daily concentrations of PM$_{2.5}$ ranged from 0-75, 75-115, 115-150, 150-250 and >250 μg/m^3 were classified as clean (C), light polluted (L), moderate polluted (M), heavy polluted (H) and serious polluted (S) periods, respectively.

3.1 The observed evidence for ammonia-rich atmosphere

The characteristics of atmospheric pollutants and meteorological parameters during the studied period were summarized in Supplement (S2.1). In this work, molar ratios of NH$_4^+$ vs. anions was used to identify the chemical species of ammonium salts (Zhou et al., 2018; Wang et al., 2021; Liu et al., 2017b; Shi et al., 2019). The calculated results (Supplement, S2.2) showed the predominant chemical species of ammonium gradually varied from the coexistence of ammonium sulfate ((NH$_4$)$_2$SO$_4$) and ammonium nitrate (NH$_4$NO$_3$) to the coexistence of ((NH$_4$)$_2$SO$_4$), NH$_4$NO$_3$ and ammonium chloride (NH$_4$Cl) with haze aggravation (Fig. S5). Further, the slope of fitted equation between excess-NH$_4^+$ and anions were still lower than 1:1 line after neutralized all the measured anions, indicating the ammonia-rich atmosphere (Fig. S5c). To meet the national demand of ultra-low emissions activities (nearly two times lower than former national standard) on gaseous pollutants, heavy usage of ammonia-containing compounds in the process of desulfurization and denitrification (Solera García et al., 2017; Tan et al., 2017) at broadly distributed thermal power plants (>300,000kWh) and the close-set coal-fired heating stations (Fig. 1) resulted ammonia fugitive provided a reasonable explanation on this ammonia-rich atmosphere. Although the retrofit of national demand of ultra-low emissions activities on gaseous pollutants (nearly two times lower than former national standard) has been completed, distributed coal-based enterprises could also emit substantial SO$_2$ and NO$_2$ and subjecting to heterogeneous reactions to further generate sulfate and nitrate and aggravated the haze events (Fig. S7a, S7b).

To show the reaction between ammonia and nitric acid and the other formation processes of nitrate in different (relative) concentrations of sulfate, the data of previous studies and different pollution levels (C, L, M, H, S) in this work were plotted in Fig. 2. When [NH$_4^+$]/[SO$_4^{2-}$] ≤ 1.5, the nitrate formation associated with crustal elements rather than ammonium; while [NH$_4^+$]/[SO$_4^{2-}$] >1.5, the homogeneous gas-phase reactions between NH$_3$ and HNO$_3$ became the major pathway for atmospheric ammonia to form NH$_4$NO$_3$ (Pathak et al., 2009; Liu et al., 2019). The results illustrated that the ammonia-rich regimes were not only found in Hohhot, but also observed in Guangzhou (Huang et al., 2011), Chengdu (Huang et al., 2018), Lanzhou USA West and East, India, Ireland, Europe, Qingdao, Italy, Lin'an (Pathak et al., 2009) in recent decades (Fig. 2). It suggested that atmospheric oxidative modifications in

210 ammonia-rich atmosphere should be a widespread atmospheric issue with significant
211 contributions on SIA generation. It was worth noting that the slopes of our data were becoming
212 steeper, coupling with the NO_3^-/SO_4^{2-} ratios change from ~4 to about 1, as the increasing
213 pollution levels. The high $PM_{2.5}$ nitrate concentration during Heavy and Serious stages cannot
214 be explained by the homogeneous gas-phase reaction involving ammonia and nitric acid, which
215 may be associating with the heterogeneous reaction in ALW on the surface of the preexisting
216 aerosols.

Fig. 2 Nitrate to sulfate molar ratio as a function of ammonium to sulfate molar ratio

217
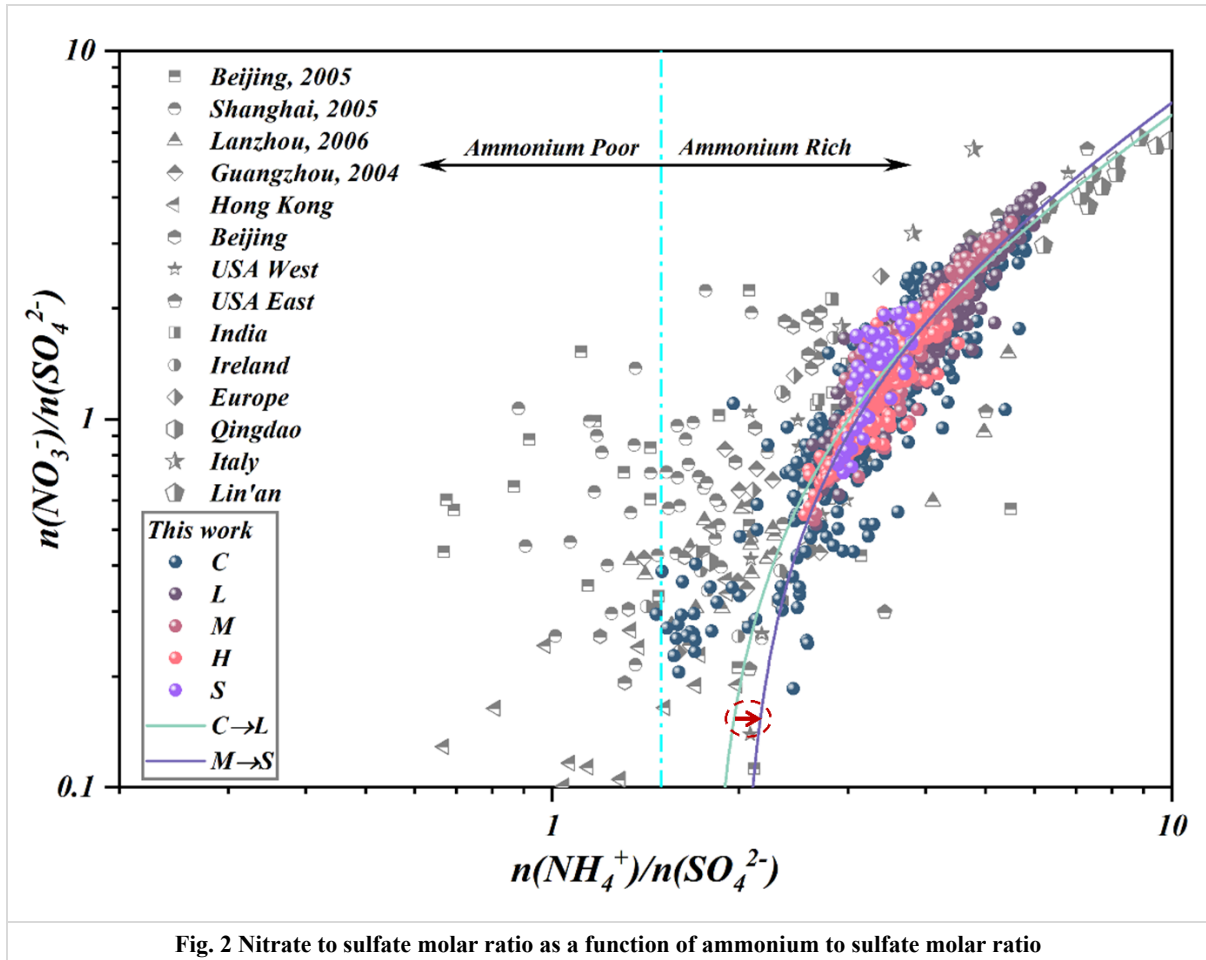
3.2 Driving mechanism of SIAs formation

3.2.1 Aerosol liquid water

220 Our results showed that SOR, NOR and SIAs in $PM_{2.5}$ presented increasing trends with the
221 increasing ALWC during the five pollution levels. The variation of predominant chemical
222 species of ammonium (Fig. 2) indicated more SIAs will be generated on particles with the
223 simultaneous increase of ALWC and $PM_{2.5}$ (Fig.3b). Theoretically, the inorganic compounds
224 conversion was enhanced via aqueous phase chemistry on moist particles owing to the
225 continuous partition of gaseous pollutants (e.g., SO_2, NO_2, N_2O_5) in ALW, then disrupted the
226 equilibrium between the gaseous and condensed phases, resulting in the aggravation of haze

events (Xue et al., 2014; Wu et al., 2018; Zheng et al., 2015b; Wang et al., 2016). Considering seasonal heating characteristics, the shift of the equilibrium between gaseous and condensed phases was enhanced with the increasing atmospheric pollutants concentrations due to the coal-fired combustion events in winter. Detailly, owing to hygroscopic nature, the particles must increase their water contents via ALW along with RH (Fig. S8a) to maintain thermodynamic equilibrium and water vapor and simultaneously enhance the oxidation and dissolution of precursors in the micro-solution (ALW) of the particulates. This process elevated the inorganic mass fraction as well as particulate mass concentrations during different pollution stages (Fig. S8b) (Bertram et al., 2009; Wang et al., 2016; Zheng et al., 2015a; Cheng et al., 2016). Due to the larger affinity of H_2SO_4 for NH_3 (aq), sulfate was preferentially and fully neutralized by ammonium in the ammonia-rich atmosphere to generate non-volatile nature of $(NH_4)_2SO_4$ (Liu et al., 2017b; Zhou et al., 2018; Wang et al., 2021). Thus, SOR presented higher exponential growth with the elevated AWLC coupling with more sulfate production (Fig. 3b). Concomitantly, the preferentially generated $(NH_4)_2SO_4$ further enhanced the hygroscopicity of particulate matter, in turn, helped more ammonia partitioning into moist particulate matter and generating ammonium salts accelerating haze aggravation (Supplement, Fig. S6, Fig. S8c). Thus, most important of all, the sharp increase of inorganic compounds associating with the elevated ALWC significantly modified the specific surface area of particulates and further accelerated the hygroscopic aerosol growth, which simultaneously provided a substrate for the ensuing heterogenous reaction and accelerated the evolution of haze events. Previous work reported that particles of different modes made different contributions to ALWC with the contributions of nuclear, Aitken, accumulation and coarse modes assessed at <1%, 3%, 85% and 12%, respectively, indicating that the contribution of accumulation mode particles to ALWC dominated among all the aerosol particle modes (Tan et al., 2017). It indicated that secondary aerosol formation mainly happens on these fine particles as the surface area and volume of the fine particles are much larger than those of the coarse particles. Thus, the observed significant correlations of ALWC with the ratios ($PM_{1.0}/PM_{2.5}$ and $PM_{2.5}/PM_{10}$) in this work also indicated that the hygroscopic growth of fine particulate matter ($D_p \leqslant 2.5um$) strongly associated with ALWC (Fig. 3a). Both the previous work and our monitoring results suggested that the ratios of $PM_{1.0}/PM_{2.5}$ and $PM_{2.5}/PM_{10}$ presented the potential possibility to index the hygroscopic growth of particulate matter.
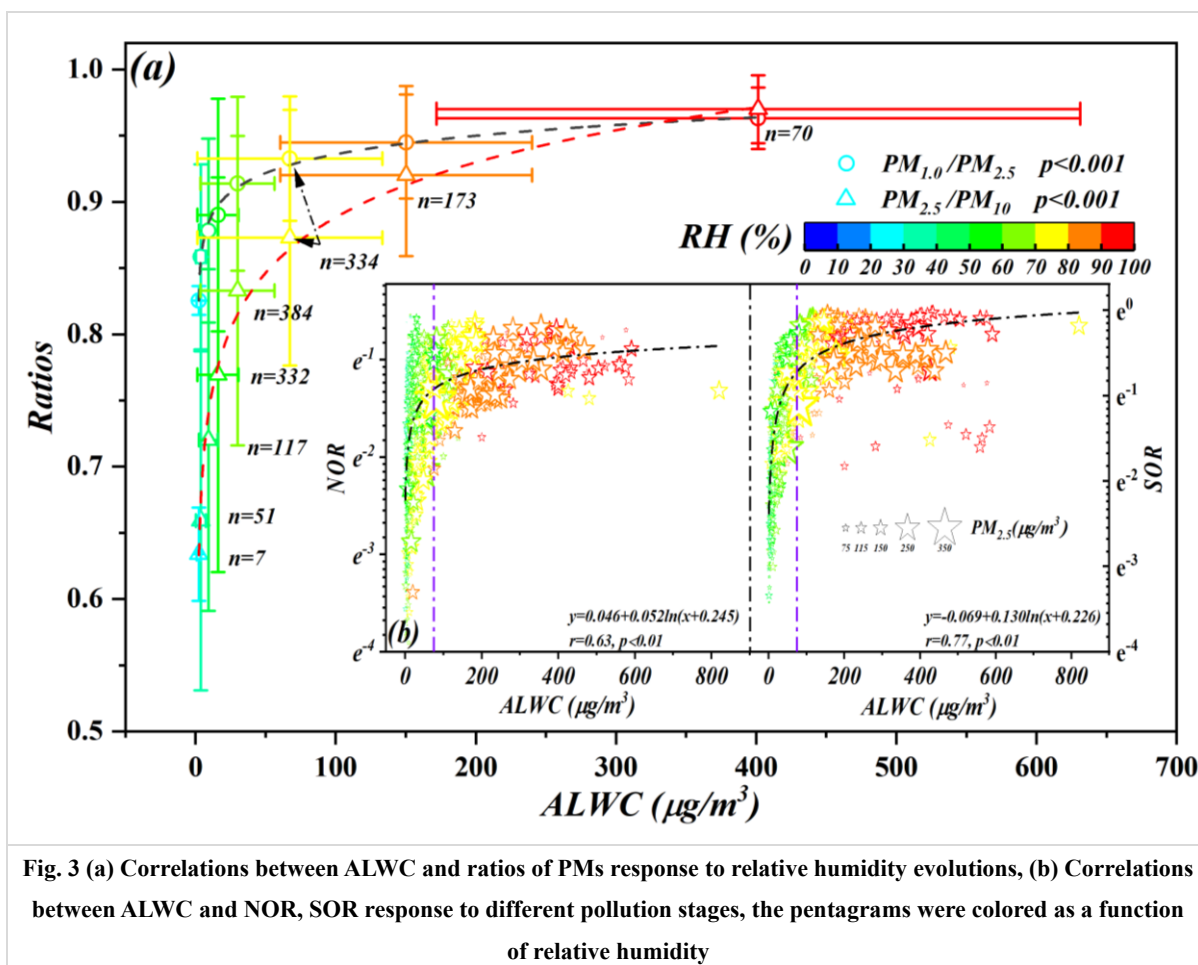
Fig. 3 (a) Correlations between ALWC and ratios of PMs response to relative humidity evolutions, (b) Correlations between ALWC and NOR, SOR response to different pollution stages, the pentagrams were colored as a function of relative humidity

3.2.2 Perturbation gases

Due to the strict control of SO_2, atmospheric concentrations of NO_2 and NH_3 gradually became as the decisive reactive precursors on regional atmospheric secondary particulate matter generation. Thus, the state-of-the-art flamework proposed by Nenes et al. (2020) was carried out to exam the chemical domain classifications and the decisive precursor based on the data sets of previous studies (Nenes et al., 2020) and this work (Fig. 4). Due to the thermodynamically stable property of the preferentially generated $(NH_4)_2SO_4$, the semi-volatile NH_4NO_3 dominate the partitioning of NH_3^T (sum of NH_3 and NH_4^+, same to NO_3^T) and NO_3^T. Although aqueous NO_3^- concentrations varied with haze processes, the calculated ε (NO_3^T) (detailed calculated method could be found in S1.2), which was an equilibrium parameter between gaseous HNO_3 and particle-phase NO_3^- (Guo et al., 2016; Fang et al., 2017), presented consistently full loadings of nitrate on the existing particulates during the studied period (Fig. S9a, Fig. S9b). This could provide clear evidence for the initial HNO_3 sensitive area and continuous control of HNO_3 during the studied periods. However, with haze aggravation, significant elevated ALWC resulted in more precursors partitioned in micro-droplets to maintain water vapor. This process induced a positive shift of HNO_3 dissolution

equilibrium and leading more HNO₃ partitioned on particles driven by the Henry's law (e.g., HNO₃(g)↔HNO₃(aq), K_H = 2.07mol/(L·Pa)). Meanwhile, HNO₃ and HONO could also produce through the reactions of $NO_2 + H_2O \xrightarrow{Het} HNO_3 + HONO$) (Huang et al., 2018). Accordingly, the OH radicals generated by HONO photolysis also contributed to this oxidation processes (Yue et al., 2020; Zhu et al., 2020). These aqueous oxidations processes were evidenced by the observation of significantly elevated HONO and PANs during the haze aggravation (Supplement, Fig. S7c, Fig. S7d). Accordingly, the equations of $NH_4^+ + NO_3^- + H^+ + OH^- \rightleftarrows NH_4NO_3 + H_2O$ and $NH_4^+ + SO_4^{2-} + H^+ + OH^- \rightarrow (NH_4)_2SO_4 + H_2O$ were shifted to generate more NH₄NO₃ and (NH₄)₂SO₄ (Nenes et al., 2020; Xie et al., 2020) due to the driving force of more ammonia partitioned in elevated ALWC (NH₃+H₂O⇌NH₃·H₂O, NH₃·H₂O⇌NH₄⁺+OH⁻). Therefore, NH₃ and NOₓ became as the decisive factors on regional atmospheric oxidability in the ammonia-rich regime (Zhai et al., 2021; Tan et al., 2017; Liu et al., 2019; Li et al., 2019).

Generally, both NH₃ and HNO₃ were the limiting factors governing the aerosol generations for cities of North China due to high loadings of atmospheric ammonia, while NH₃ governed PM formation for the southeast US (SAS) (Zhao et al., 2020). Thanks to the raw data of Shenzhen (SZ) (Wang et al., 2022), we also calculated the ALWC and aerosol pH using ISORROPIA-II and the scatters of SZ suggested obvious chemical transition from HNO₃-NH₃ regime to NH₃ sensitive regime due to the differently originated air masses. Although both cities located in US, the findings in California (CNX) were quite interesting and distributed in the insensitive region and the combined NH₃-HNO₃ sensitive region due to the moderate NH₃ levels and the complicated atmospheric conditions during the observation (Nenes et al., 2020). In our work, the data points (541/744) in summer (pH=3.47±1.29) mostly lied in HNO₃ sensitive region, while chemical domains of perturbation gas limiting the generation of secondary particulate matters presented obvious shifts from HNO₃ sensitive to HNO₃ and NH₃ co-sensitive regime with the haze aggravation in winter. Some data points of this work lied in the combined NH₃-HNO₃ region in winter owing to the more acidic condition. Under the stable pH of aerosols in winter at Hohhot (pH=4-5), the more important is that a fraction of points will distribute in the combined NH₃-HNO₃ region when ALWC>75 μg/m³, which may be attributed to the aqueous chemical transformation driven by Henry's law mentioned above due to the elevating ALWC. Comparatively, the aerosols pH in summer was significantly lower than those in winter in Hohhot. Compared to TJ and SZ, the aerosols pH of Hohhot in winter was also significantly higher (Fig. 4) due to the acidity of atmospheric PM is largely depended on the alkaline material in surface soils in arid and semi-arid region and the elevated

309   atmospheric ammonia. In terms of seasonal characteristics, the higher temperature in summer

310   elevates the volatility of NH_4NO_3 and dominates the partitioning of NH_3^T in atmospheric phase

311   to decrease the pH of aerosols. Therefore, as can be seen from Fig. 4, the data points measured

312   in winter Hohhot characterized as higher pH and low ALWC than those in summer (Hohhot,

313   SAS, CNX, SZ). According to the framework of Nenes et al. (2020), the transition points of

314   Hohhot (whether winter or summer) between NH_3-dominated and HNO_3-dominated sensitivity

315   also occurs at a pH around 2 but at lower levels of ALWC. Theoretically, it should be associated

316   with the more aridity of Hohhot locating in the arid and semi-arid region of China. Our results

317   provided the evidence for "the additional insight" proposed by Nenes et al. (2020) that the

318   transition ALWC varies with season change and the aridity of sites, in response to seasonal

319   variability and climate change. Although this effort could provide sound explanation for

320   limiting gaseous pollutants on PM formation, mechanisms on their chemical domains,

321   especially the roles of ALW in different locations with various conditions need further study in

322   the future.

Fig. 4 Chemical domains of aerosol response to ammonia and nitrate emissions
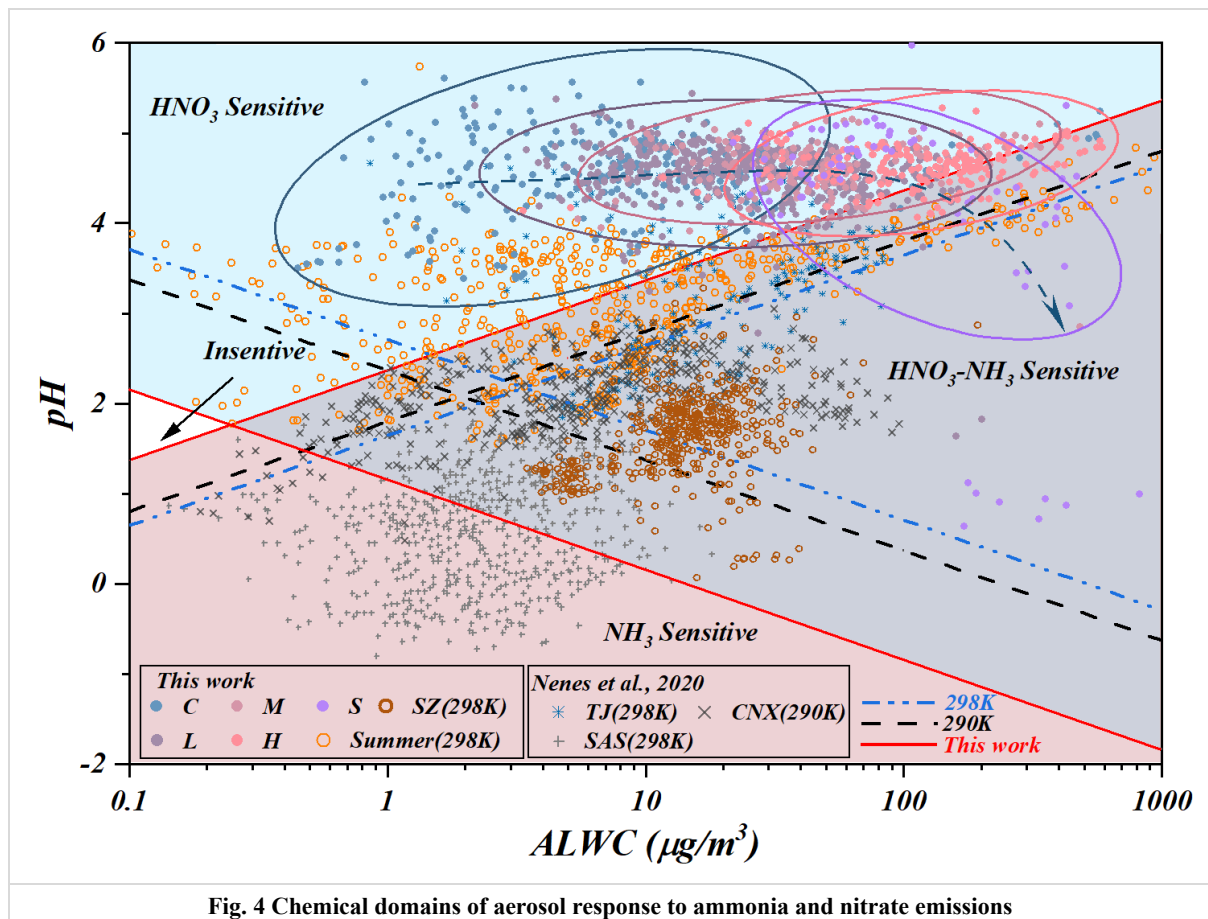
323   *3.2.3 The shifting of SIAs formation mechanism driven by ALW*

324   It's worth noting that two independent correlations were found between SOR and odd oxygen

325   (O_x, O_x=NO_2+O_3) during the aggravating processes of haze events, indicating the differential

mechanisms of atmospheric oxidability on sulfate generations at different stages (Fig. 5a). Different to inefficient homogeneous sulfate oxidation efficiency (Supplement, Fig. S10), significant correlations pairs of NO_2 with SOR (Fig.5b) and NOR with SO_4^{2-} (Fig.5c) suggested the haze aggravation was largely related to the regional NO_2 levels due to the regulating effects on atmospheric oxidizability. Thus, the aqueous-phase oxidation of S(IV) by NO_2 (aq) was triggered and accelerated by the increasing ALWC and the following equation (Yao et al., 2020; Wang et al., 2016) (Supplement, Fig. S11a):

$$S(IV) + NO_2(aq) + H_2O \rightarrow S(VI) + H^+ + NO_2^- \qquad (R1)$$
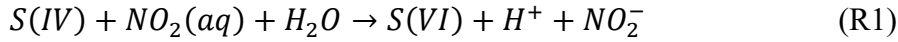
Meanwhile, sharp logarithmic increase between SOR and NH_4^+ were also observed from Clean to Moderate pollution stages (Supplement, Fig. S12). Due to the joint effects of ammonia-rich atmosphere and ammonia's extremely water-soluble property, sufficient hydroxide generated by ammonia dissolution forced the NO_2 partitioned in ALW to maintain pH through neutralization and producing sulfate via R1. Thus, the following equation (R2) was derived with considering the processes of ammonia hydrolysis, which was evidenced by Fig. S11b.

$$S(IV) + NO_2(aq) + NH_3(aq) + H_2O \rightarrow S(VI) + NH_4^+ + NO_2^- + H^+ + NO_3^- \quad (R2)$$
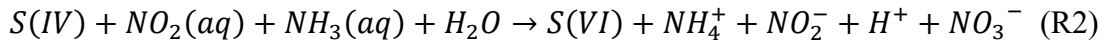
Generally, NOR<0.1 means insignificant nitrogen oxide oxidation, therefore the observed regime shift of nitrate and ammonia chemical behavior on sulfate generation suggested the sulfate generation was preferentially triggered by the high ammonia utilization, then accelerated by the co-effects of ammonia utilization and nitrogen oxide oxidation (Fig. 5c).

Fig. 5 Correlations between (a) O_x and SOR, (b) NO_2 and SOR, (c) NOR and SO_4^{2-}
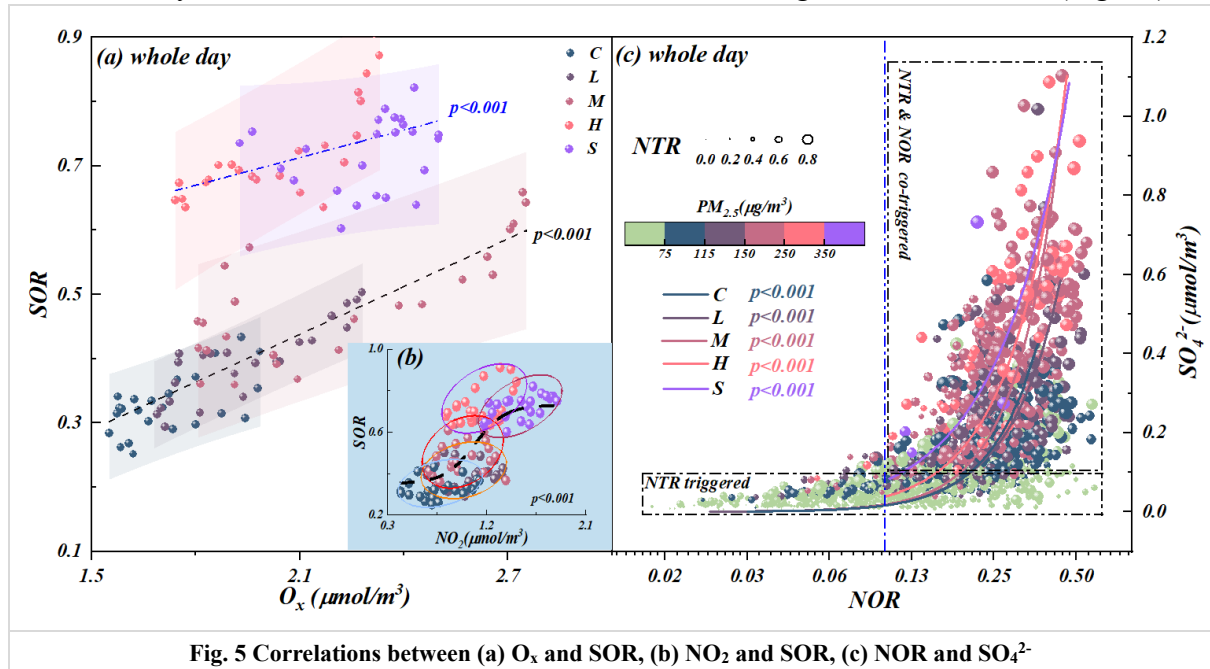
Accordingly, the reaction R2 was activated due to the increased ALWC forced more ammonia to partition into moist particulate matter driven by the Henry's law in the ammonia-rich atmosphere ($NH_{3(g)} \rightarrow NH_{3(aq)}$) (Supplement, Fig. S9c) (Clegg et al., 1998; Wu et al., 2018;

348   Xie et al., 2020). Meanwhile, our calculated aqueous generated NO_3^- nicely matched theoretical

349   nitrate aqueous generation curve (the solid blue line in Fig. S9b) proposed by Guo et al. (2017),

350   suggesting the pathway of fast sulfate formation from oxidation of S(IV) by NO_2 to generate

351   HONO (Wang et al., 2020) (Supplement, Fig. S11) via the reaction R2. As a result, the

352   thermodynamically stable $(NH_4)_2SO_4$ would be preferentially formed to maintain its water

353   vapor pressure and thermodynamic equilibrium, then trigged the haze formation. Thus, the

354   mentioned effects resulted in a pronounced increase of NH_3 partitioning with the haze

355   aggravation, suggesting the importance of ammonia partition on sulfate generations, namely,

356   NTR-controlled regime with ALWC<75 μg/m^3. In summary, when ALWC<75 μg/m^3, the

357   sulfate generation was preferentially triggered by high ammonia utilization, then accelerated

358   by nitrogen oxide oxidation from Clean to Light pollution stages (Fig. 5c) with NOR<0.3,

359   SOR<0.4 and NTR<0.7. In this period, the chemical composition of SIAs characterized as the

360   moral ratio of $NO_3^-:SO_4^{2-}$=2:1 (Fig. 6).

361   When ALWC>75μg/m^3, the haze was aggravated from Moderate to Serious stages along

362   with the increasing ALWC. As a result of increase in ALW, large amount of H^+ was dissociated

363   during the generation of ammonium sulfate (Supplement, Fig. S13a). From Light to Moderate

364   pollution stages, the solubility SO_2 driven by Henry's law was self-limiting due to the acidity

365   effect in low ALWC (with ALWC<75 μg/m^3). Therefore, low sulfate concentrations coupled

366   with low ALWC at the beginning of haze event (Supplement, Fig. S13a). However, due to the

367   co-effects of elevated ALWC and hygroscopic nature of pre-generated ammonia sulfate, H^+

368   concentrations were diluted and nearly constant in-situ pH with the increase of ALWC during

369   Heavy and Serious pollution stages (Supplement, Fig. S14) (Wang et al., 2016; Clifton et al.,

370   1988; Huie and Neta, 1986; Lee and Schwartz, 1982). Hence, the significantly elevated ALWC

371   provided more chance for the partition of SO_2, NO_2 and NH_3 in ALW from Moderate to Serious

372   pollution stages. Theoretically, Henry's constants of NO_2 (9.74×10^{-8} mol·(L·Pa)$^{-1}$) is 3-4 orders

373   of magnitude lower than those of SO_2 (1.22×10^{-5} mol·(L·Pa)$^{-1}$) and NH_3 (6.12×10^{-4}

374   mol·(L·Pa)$^{-1}$), however, it is worth noting that the aqueous generated NO_3^- from Moderate to

375   Serious stages rapidly increased 2-5 times higher than Clean and Light stages (Supplement,

376   Fig. S9b). Meanwhile, according to our monitoring results, the solar spectrophotometry at

377   380nm during Moderate to Serious stages was significantly lower than that in Clean stage

378   (Supplement, Fig. S15), suggesting the aqueous oxidation of NO_2 was the predominant

379   compared to chain photolysis (Huang et al., 2018). Accordingly, it could be deduced that

380   aqueous-phase chemistry reaction of SO_2 and NH_3 in ALW, driven by Henry law, became the

381   dominant mechanism for sulfate formation due to more NO_2 was required to take part in the

382 fast sulfate formation with the increase of ALWC in the ammonia-rich atmosphere by the
383 reaction R2. Thus, with the increasing of ALWC, high concentrations of sulfate and nitrate with
384 high SOR (0.5-0.9), NOR (0.3-0.5) and NTR (>0.7) induced the haze events becoming Heavy
385 and Serious levels (Fig. 5c). Simultaneously, the calculated heterogeneous sulfate production
386 rate (Jacob, 2000; Mcneill, 2015) (Supplement, Fig. S16) presented similar trends with the
387 impacts of ammonia on sulfate production during different pollution stages (Xue et al., 2016;
388 Cheng et al., 2016; Liu et al., 2020). It further stated the environmental significance of the
389 partitioning of SO_2 and NH_3 between gas and aqueous (ALW) phases for SIAs formation and
390 haze aggravation. Our results provided the evidence of significant negative correlations
391 between HONO and N_2O (Supplement, Fig. S17) from Moderate to Serious stages and positive
392 correlations between HONO and SOR (Supplement, Fig.S11a), highlighting the recent reported
393 secondary aqueous-phase oxidation pathway of SO_2 by HONO from moderate pollution period
394 $(2N(III) + 2S(IV) \rightarrow N_2O \uparrow +2S(VI) + other\ products)$ (Wang et al., 2020). In summary,
395 when ALWC>75 μg/m^3, aqueous-phase chemistry reaction of SO_2 and NH_3 in ALW became
396 the prerequisite for SIAs formation driven by Henry's law in the ammonia-rich atmosphere
397 during Heavy and Serious stages with high SOR (0.5-0.9), NOR (0.3-0.5), NTR (>0.7). In this
398 period, the chemical composition of SIAs characterized as the moral ratio of $NO_3^-:SO_4^{2-}=1:1$
399 (Fig. 6).
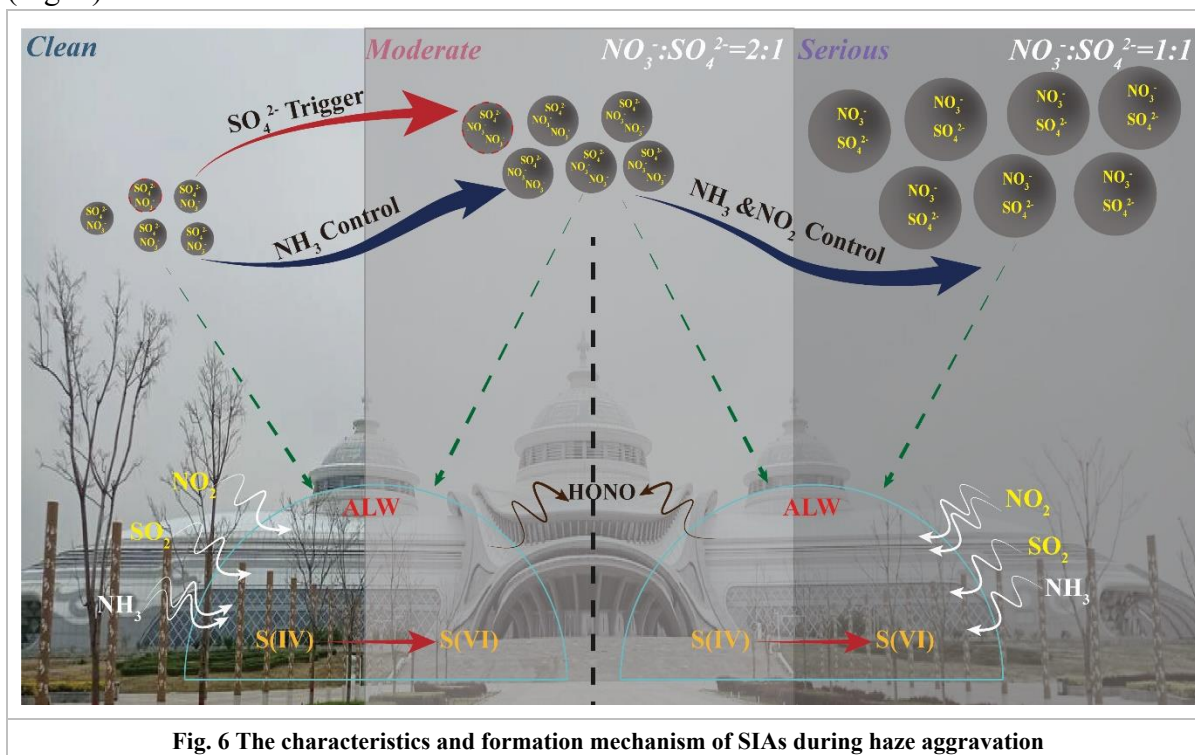
Fig. 6 The characteristics and formation mechanism of SIAs during haze aggravation

400

3.2.4 The positive feedback of sulfate on nitrate production

Previous works suggested that the homogeneous reaction of NO_2 with OH radicals during daylight and heterogeneous hydrolysis of N_2O_5 at night were the main routes on nitrate formation during haze episodes (He et al., 2018; Liu et al., 2020; Liu et al., 2019). Unsurprising, higher nitrate production rates (ΔNO_3^-, the difference of hour concentrations and matrixing afterwards) were frequently observed in ammonia-rich conditions due to that ammonia-rich regime was more conducive on nitrate generation. However, the high level of nitrate production rates (ΔNO_3^-) were found in the area characterizing as high ammonium and low sulfate levels, suggesting that highly utilizing ammonium and pre-generated sulfate promoting particle-phase nitrate generations (Fig. 7).

Fig. 7 Direct observation of nitrate production facilitated by initially generated sulfate.
(All data were matrixed to avoid interference caused by dimensionality)
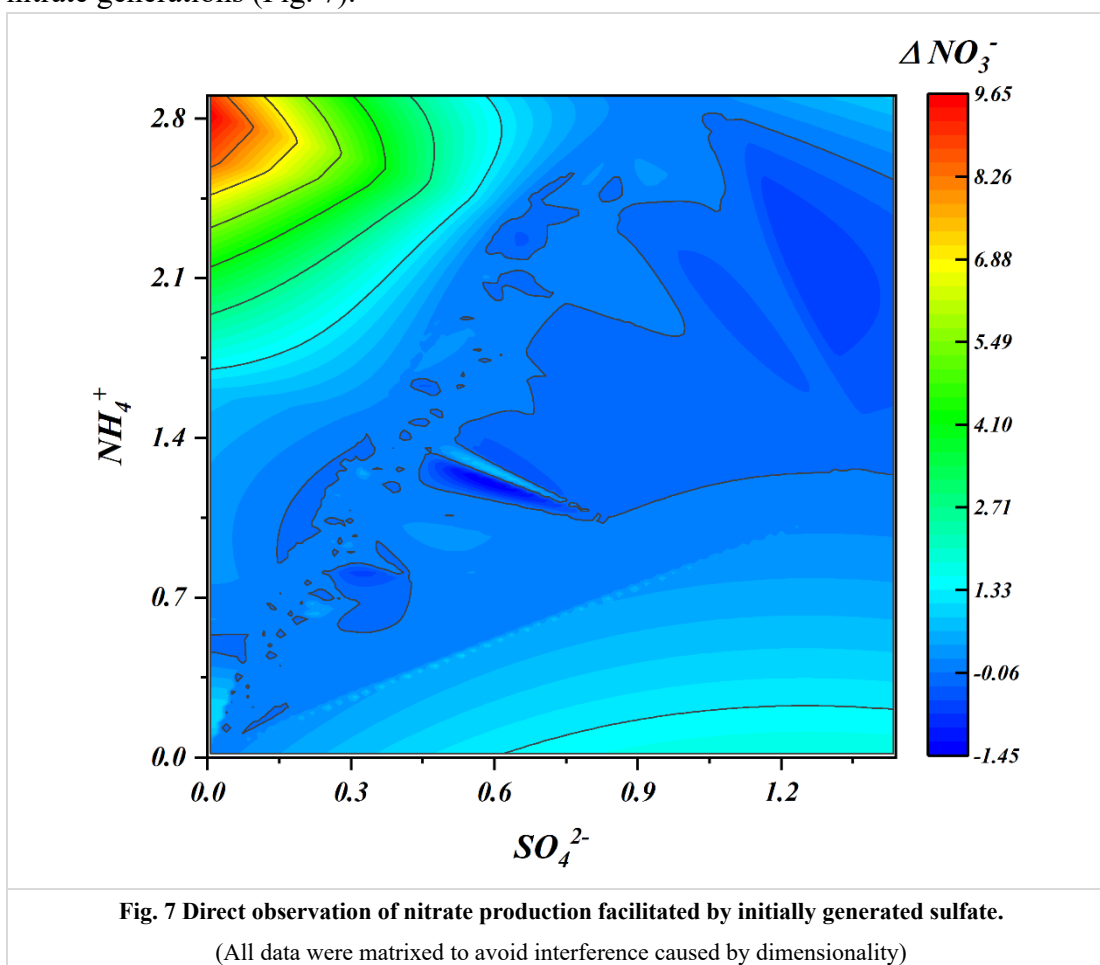
Here, we proposed a hypothesis about the hydrogen ion concentration to respond the above observations. As is known to all, apart from the extremely low levels of crustal elements, ammonia is the only alkaline gas to neutralize the acidic gases in the atmosphere and generate ammonium ions (Xie et al., 2020). Thus, the concentrations of particulate sulfate and nitrate are affected by the partitioning of NH_4^+/NH_3. Thereby, higher values of ΔNO_3^- and ΔSO_4^{2-}

always occurred in the regions with higher ammonium ions were not confused (Fig. 7, Fig. S18). According to both our results and published laboratory work (Wang et al., 2016), the acidity of the particulate matter could be significantly modified by the bulk aqueous reaction between NO_2 and SO_2, in which this reaction could be further enhanced due to in the presence of NH_3. As a result of the increase in RH, the partitioning of atmospheric ammonia was broken in a deep extent, which enhanced the neutralization of S(VI) by ammonia at the particle surface to generate ammonium sulfate and dissociate huge H^+ (Fig. S13b, red part). Simultaneously, the ALWC did not raised significantly (Fig. S14b) at the beginning of haze event with relative low sulfate concentrations. Thus, hydrogen ions generated from sulfate dissociation absorb ammonia more effectively from the ammonia-rich atmosphere at low relative humidity during the early pollution stages, which significantly promotes the net nitrate production. However, due to the co-effects of elevated RH and hygroscopic nature of pre-generated ammonia sulfate, H^+ concentrations were diluted and shown as nearly constant in-situ pH (Fig. S14a). According to previous works, the reaction between firstly generated sulfate and bisulfate with ammonia were treated as the determination reaction on particle acidity (Weber et al., 2016; Liu et al., 2017a). This reaction is self-limiting due to the acidity effect, namely that it increases the acidity of aqueous phase and in turn reduces the efficiency of Henry's constant for SO_2 solubility and reaction rate and reduced the H^+ formation rates from moderate periods, compared with clean periods (Fig. S13b, blue) (Wang et al., 2016; Clifton et al., 1988; Huie and Neta, 1986; Lee and Schwartz, 1982). Due to the co-effects of RH increase and hygroscopic of sulfate, the ALWC was significantly elevated with the worsen of haze. Although more H^+ was generated in this process, no significant decrease in pH was found with the haze aggravation due to the dilution effect of ALWC on H^+. Previous works suggested that in the case of ALWC increase, nitrate production is controlled by elevated H^+ associating with the increase of sulfate, namely, NO_3^- presented elevating trend with the increases of H^+ concentration (Xie et al., 2020). Thus, although H^+ from the dissociation of sulfuric acid and full-loaded particle nitrate in conjunction with the haze aggravation generate particle HNO_3 (Fig. S19a) could forcing more ammonia partitioned on the particles to generate ammonium nitrate (Fig. S19b), net nitrate production (ΔNO_3^-) was nearly consistent.

4 Conclusions

The formation of SIAs, especially sulfates and nitrates, was inherently associated with ALWC during the haze aggravation, in which the roles of ALWC should be more significant in ammonia-rich atmosphere. The novelty of our work is to find the shifting of secondary inorganic aerosols formation mechanism during haze aggravation and explain the different

roles of ALWC in a broader scale ($\sim$500 ug/m^3) in ammonia-rich atmosphere based on the in-situ high-resolution on-line monitoring data sets. The results showed that chemical domains of perturbation gas limiting the generation of secondary particulate matters presented obvious shifts from HNO$_3$ sensitive to HNO$_3$ and NH$_3$ co-sensitive regime with the haze aggravation, indicating the powerful driving effects of ammonia in ammonia-rich atmosphere. When ALWC<75 ug/m^3, the sulfate generation was preferentially triggered by the high ammonia utilization, then accelerated by nitrogen oxide oxidation from Clean to Moderate pollution stages, characterizing as NOR<0.3, SOR<0.4, NTR<0.7 and the moral ratio of NO$_3^-$:SO$_4^{2-}$=2:1. While ALWC>75 ug/m^3, aqueous-phase chemistry reaction of SO$_2$ and NH$_3$ in ALW became the prerequisite for SIAs formation driven by Henry's law in the ammonia-rich atmosphere during Heavy and Serious stages, characterizing as high SOR (0.5-0.9), NOR (0.3-0.5), NTR (>0.7) and the moral ratio of NO$_3^-$:SO$_4^{2-}$=1:1. A positive feedback of sulfate on nitrate production was also observed in this work. Our work provides a potential explanation for the interactive mechanism and feedback between nitric aqueous chemistry and sulfate formation in ammonia-rich atmosphere based on high-resolution field observation. It implies the target controlling of haze should not simply focus on SO$_2$ and NO$_2$, more attention should be paid on gaseous precursors (e.g., SO$_2$, NO$_2$, NH$_3$) and aerosol chemical constitution during different haze stages.

Data availability. All data of this study are available from the corresponding author upon reasonable request (lcw2008@imu.edu.cn).

Supplement. The Supplement related to this article is available online at

Author Contributions. FX: Data curation, Formal analysis, Software, Writing-original draft. YS: Investigation, Formal analysis. YLT: Methodology, Software. YSH: Investigation, Formal analysis. XJZ: Investigation, Formal analysis, Software. PW: Methodology, Investigation. RHY: Software, Writing-review & editing. WW: Investigation, Validation, Writing-review & editing. JH: Investigation, Methodology. JYX: Investigation, Validation, Supervision, Writing-review & editing. CWL: Initiating and leading this research, Supervision, Writing-review & editing.

Competing interest. The authors declared that they have no conflict of interest.

Acknowledgments. This work is supported by Science and Technology Major Project on Air Pollution Prevention and Prediction in Hohhot-Baotou-Ordos Cities Group of Inner Mongolia (No. 2020ZD0013), National Natural Science Foundation of China (No. 42167028, 41763014) and Science Fund for Distinguished Young Scholars of Inner Mongolia (2019JQ05).

References

Ansari, A. S. and Pandis, S. N.: Water Absorption by Secondary Organic Aerosol and Its Effect on Inorganic Aerosol Behavior, Environ. Sci. Technol., 34, 71-77, 10.1021/es990717q, 2000.

Bertram, T. H., Thornton, J. A., Riedel, T. P., Middlebrook, A. M., Bahreini, R., Bates, T. S., Quinn, P. K., and Coffman, D. J.: Direct observations of N_2O_5 reactivity on ambient aerosol particles, Geophys. Res. Lett., 36, https://doi.org/10.1029/2009GL040248, 2009.

Bian, Y. X., Zhao, C. S., Ma, N., Chen, J., and Xu, W. Y.: A study of aerosol liquid water content based on hygroscopicity measurements at high relative humidity in the North China Plain Atmos. Chem. Phys., 14, 6417–6426, https://doi.org/10.5194/acp-14-6417-2014, 2014.

Carlton, A. and Turpin, B.: Particle partitioning potential of organic compounds is highest in the Eastern US and driven by anthropogenic water, Atmos. Chem. Phys., 13, 10203-10214, 2013.

Cheng, Y., Zheng, G., Wei, C., Mu, Q., Zheng, B., Wang, Z., Gao, M., Zhang, Q., He, K., Carmichael, G., Pöschl, U., and Su, H.: Reactive nitrogen chemistry in aerosol water as a source of sulfate during haze events in China, Sci. Adv., 2, e1601530, 10.1126/sciadv.1601530, 2016.

Clegg, S. L., Brimblecombe, P., and Wexler, A. S.: Thermodynamic Model of the System $H^+-NH_4^+-SO_4^{2-}-NO_3^-$$-H_2O$ at Tropospheric Temperatures, J. Phys. Chem. A, 102, 2137-2154, 10.1021/jp973042r, 1998.

Clifton, C. L., Altstein, N., and Huie, R. E.: Rate constant for the reaction of nitrogen dioxide with sulfur(IV) over the pH range 5.3-13, Environ. Sci. Technol., 22, 586-589, 10.1021/es00170a018, 1988.

Davies, J. F. and Wilson, K. R.: Nanoscale interfacial gradients formed by the reactive uptake of OH radicals onto viscous aerosol surfaces, Chem. Sci., 6, 7020-7027, 10.1039/C5SC02326B, 2015.

Fang, T., Guo, H., Zeng, L., Verma, V., Nenes, A., and Weber, R. J.: Highly Acidic Ambient Particles, Soluble Metals, and Oxidative Potential: A Link between Sulfate and Aerosol Toxicity, Environ. Sci. Technol., 51, 2611-2620, 10.1021/acs.est.6b06151, 2017.

Fu, H. and Chen, J.: Formation, features and controlling strategies of severe haze-fog pollutions in China, Sci. Total Environ., 578, 121-138, https://doi.org/10.1016/j.scitotenv.2016.10.201, 2017.

Gao, J., Wei, Y., Shi, G., Yu, H., Zhang, Z., Song, S., Wang, W., Liang, D., and Feng, Y.: Roles of RH, aerosol pH and sources in concentrations of secondary inorganic aerosols, during different pollution periods, Atmos. Environ., 241, 117770, https://doi.org/10.1016/j.atmosenv.2020.117770, 2020.

Ge, B., Xu, X., Ma, Z., Pan, X., Wang, Z., Lin, W., Ouyang, B., Xu, D., Lee, J., Zheng, M., Ji, D., Sun, Y., Dong, H., Squires, F. A., Fu, P., and Wang, Z.: Role of Ammonia on the Feedback Between AWC and Inorganic Aerosol Formation During Heavy Pollution in the North China Plain, Earth Space Sci., 6, 1675-1693, https://doi.org/10.1029/2019EA000799, 2019.

Guo, H., Liu, J., Froyd, K. D., Roberts, J. M., Veres, P. R., Hayes, P. L., Jimenez, J. L., Nenes, A., and Weber, R. J.: Fine particle pH and gas–particle phase partitioning of inorganic species in Pasadena, California, during the 2010 CalNex campaign, Atmos. Chem. Phys., 17, 5703-5719, 10.5194/acp-17-5703-2017, 2017.

Guo, H., Sullivan, A. P., Campuzano-Jost, P., Schroder, J. C., Lopez-Hilfiker, F. D., Dibb, J. E., Jimenez, J. L., Thornton, J. A., Brown, S. S., Nenes, A., and Weber, R. J.: Fine particle pH and the partitioning of nitric

527   acid during winter in the northeastern United States, J. Geophys. Res.: Atmos.

528   , 121, 10,355-310,376, https://doi.org/10.1002/2016JD025311, 2016.

529 Guo, S., Hu, M., Zamora, M. L., Peng, J., Shang, D., Zheng, J., Du, Z., Wu, Z., Shao, M., Zeng, L., Molina, M.

530   J., and Zhang, R.: Elucidating severe urban haze formation in China, Proc. Natl. Acad. Sci. USA, 111,

531   17373-17378, 10.1073/pnas.1419604111, 2014.

532 Gwynn, R. C., Burnett, R. T., and Thurston, G. D.: A time-series analysis of acidic particulate matter and daily

533   mortality and morbidity in the Buffalo, New York, region, Environ. Health Persp., 108, 125-133,

534   doi:10.1289/ehp.00108125, 2000.

535 He, P., Xie, Z., Chi, X., Yu, X., Fan, S., Kang, H., Liu, C., and Zhan, H.: Atmospheric $\Delta 17O(NO3^-)$ reveals

536   nocturnal chemistry dominates nitrate production in Beijing haze, Atmos. Chem. Phys., 18, 14465-14476,

537   10.5194/acp-18-14465-2018, 2018.

538 Hodas, N., Sullivan, A. P., Skog, K., Keutsch, F. N., Collett, J. L., Decesari, S., Facchini, M. C., Carlton, A. G.,

539   Laaksonen, A., and Turpin, B. J.: Aerosol Liquid Water Driven by Anthropogenic Nitrate: Implications for

540   Lifetimes of Water-Soluble Organic Gases and Potential for Secondary Organic Aerosol Formation, Environ.

541   Sci. Technol., 48, 11127-11136, 10.1021/es5025096, 2014.

542 Huang, R.-J., Duan, J., Li, Y., Chen, Q., Chen, Y., Tang, M., Yang, L., Ni, H., Lin, C., Xu, W., Liu, Y., Chen, C.,

543   Yan, Z., Ovadnevaite, J., Ceburnis, D., Dusek, U., Cao, J., Hoffmann, T., and O'Dowd, C. D.: Effects of

544   NH_3 and alkaline metals on the formation of particulate sulfate and nitrate in wintertime Beijing, Sci. Total

545   Environ., 717, 137190, https://doi.org/10.1016/j.scitotenv.2020.137190, 2020.

546 Huang, R.-J., Zhang, Y., Bozzetti, C., Ho, K.-F., Cao, J.-J., Han, Y., Daellenbach, K. R., Slowik, J. G., Platt, S. M.,

547   Canonaco, F., Zotter, P., Wolf, R., Pieber, S. M., Bruns, E. A., Crippa, M., Ciarelli, G., Piazzalunga, A.,

548   Schwikowski, M., Abbaszade, G., Schnelle-Kreis, J., Zimmermann, R., An, Z., Szidat, S., Baltensperger, U.,

549   Haddad, I. E., and Prévôt, A. S. H.: High secondary aerosol contribution to particulate pollution during haze

550   events in China, Nature, 514, 218-222, 10.1038/nature13774, 2014.

551 Huang, X., Qiu, R., Chan, C. K., and Ravi Kant, P.: Evidence of high $PM_{2.5}$ strong acidity in ammonia-rich

552   atmosphere of Guangzhou, China: Transition in pathways of ambient ammonia to form aerosol ammonium

553   at $[NH_4^+]/[SO_4^{2-}]$=1.5, Atmos. Res., 99, 488-495, https://doi.org/10.1016/j.atmosres.2010.11.021, 2011.

554 Huang, X., Zhang, J., Luo, B., Wang, L., Tang, G., Liu, Z., Song, H., Zhang, W., Yuan, L., and Wang, Y.: Water-

555   soluble ions in $PM_{2.5}$ during spring haze and dust periods in Chengdu, China: Variations, nitrate formation

556   and potential source areas, Environ. Pollut., 243, 1740-1749, https://doi.org/10.1016/j.envpol.2018.09.126,

557   2018.

558 Huie, R. E. and Neta, P.: Kinetics of one-electron transfer reactions involving chlorine dioxide and nitrogen

559   dioxide, J. Phys. Chem., 90, 1193-1198, 10.1021/j100278a046, 1986.

560 Jacob, D. J.: Heterogeneous chemistry and tropospheric ozone, Atmos. Environ., 34, 2131-2159,

561   https://doi.org/10.1016/S1352-2310(99)00462-8, 2000.

562 Jin, X., Wang, Y., Li, Z., Zhang, F., Xu, W., Sun, Y., Fan, X., Chen, G., Wu, H., Ren, J., Wang, Q., and Cribb, M.:

563   Significant contribution of organics to aerosol liquid water content in winter in Beijing, China, Atmos. Chem.

564   Phys., 20, 901–914, https://doi.org/10.5194/acp-20-901-2020, 2020.

565 Kanchan, K., Gorai, A. K., and Goyal, P.: A review on air quality indexing system, Asian J Atmos. Enviro., 9,

566   101-113, 2015.

567 Lavigne, E., Yasseen, A. S., Stieb, D. M., Hystad, P., van Donkelaar, A., Martin, R. V., Brook, J. R., Crouse, D.

568   L., Burnett, R. T., Chen, H., Weichenthal, S., Johnson, M., Villeneuve, P. J., and Walker, M.: Ambient air

569   pollution and adverse birth outcomes: Differences by maternal comorbidities, Enviro. Res., 148, 457-466,

570   https://doi.org/10.1016/j.envres.2016.04.026, 2016.

Lee, Y. and Schwartz, S.: Kinetics of oxidation of aqueous sulfur (IV) by nitrogen dioxide, Elsevier, New York, pp 453-466 pp.1982.

Li, H., Cheng, J., Zhang, Q., Zheng, B., Zhang, Y., Zheng, G., and He, K.: Rapid transition in winter aerosol composition in Beijing from 2014 to 2017: response to clean air actions, Atmos. Chem. Phys., 19, 11485-11499, 10.5194/acp-19-11485-2019, 2019.

Liu, M., Song, Y., Zhou, T., Xu, Z., Yan, C., Zheng, M., Wu, Z., Hu, M., Wu, Y., and Zhu, T.: Fine particle pH during severe haze episodes in northern China, Geophys. Res. Lett., 44, 5213-5221, https://doi.org/10.1002/2017GL073210, 2017a.

Liu, M., Huang, X., Song, Y., Tang, J., Cao, J., Zhang, X., Zhang, Q., Wang, S., Xu, T., Kang, L., Cai, X., Zhang, H., Yang, F., Wang, H., Yu, J. Z., Lau, A. K. H., He, L., Huang, X., Duan, L., Ding, A., Xue, L., Gao, J., Liu, B., and Zhu, T.: Ammonia emission control in China would mitigate haze pollution and nitrogen deposition, but worsen acid rain, Proc. Natl. Acad. Sci. USA, 116, 7760-7765, 10.1073/pnas.1814880116, 2019.

Liu, P., Ye, C., Xue, C., Zhang, C., Mu, Y., and Sun, X.: Formation mechanisms of atmospheric nitrate and sulfate during the winter haze pollution periods in Beijing: gas-phase, heterogeneous and aqueous-phase chemistry, Atmos. Chem. Phys., 20, 4153-4165, 10.5194/acp-20-4153-2020, 2020.

Liu, T., Chan, A. W. H., and Abbatt, J. P. D.: Multiphase Oxidation of Sulfur Dioxide in Aerosol Particles: Implications for Sulfate Formation in Polluted Environments, Environ. Sci. Technol., 55, 4227-4242, 10.1021/acs.est.0c06496, 2021.

Liu, Z., Xie, Y., Hu, B., Wen, T., Xin, J., Li, X., and Wang, Y.: Size-resolved aerosol water-soluble ions during the summer and winter seasons in Beijing: Formation mechanisms of secondary inorganic aerosols, Chemosphere, 183, 119-131, https://doi.org/10.1016/j.chemosphere.2017.05.095, 2017b.

McNeill, V. F.: Aqueous Organic Chemistry in the Atmosphere: Sources and Chemical Processing of Organic Aerosols, Environ. Sci. Technol., 49, 1237-1244, 10.1021/es5043707, 2015.

Nenes, A., Pandis, S. N., Weber, R. J., and Russell, A.: Aerosol pH and liquid water content determine when particulate matter is sensitive to ammonia and nitrate availability, Atmos. Chem. Phys., 20, 3249-3258, 10.5194/acp-20-3249-2020, 2020.

Nguyen, T., Petters, M., Suda, S., Guo, H., Weber, R., and Carlton, A.: Trends in particle-phase liquid water during the Southern Oxidant and Aerosol Study, Atmos. Chem. Phys., 14, 10911-10930, 2014.

Nie, W., Ding, A. J., Xie, Y. N., Xu, Z., Mao, H., Kerminen, V. M., Zheng, L. F., Qi, X. M., Huang, X., Yang, X. Q., Sun, J. N., Herrmann, E., Petäjä, T., Kulmala, M., and Fu, C. B.: Influence of biomass burning plumes on HONO chemistry in eastern China, Atmos. Chem. Phys., 15, 1147-1159, 10.5194/acp-15-1147-2015, 2015.

Nozière, B., Dziedzic, P., and Córdova, A.: Inorganic ammonium salts and carbonate salts are efficient catalysts for aldol condensation in atmospheric aerosols, Phys. Chem. Chem. Phys., 12, 3864-3872, 10.1039/B924443C, 2010.

Pathak, R. K., Wu, W. S., and Wang, T.: Summertime $PM_{2.5}$ ionic species in four major cities of China: nitrate formation in an ammonia-deficient atmosphere, Atmos. Chem. Phys., 9, 1711-1722, 10.5194/acp-9-1711-2009, 2009.

Rumsey, I. C., Cowen, K. A., Walker, J. T., Kelly, T. J., Hanft, E. A., Mishoe, K., Rogers, C., Proost, R., Beachley, G. M., Lear, G., Frelink, T., and Otjes, R. P.: An assessment of the performance of the Monitor for AeRosols and GAses in ambient air (MARGA): a semi-continuous method for soluble compounds, Atmos. Chem. Phys., 14, 5639-5658, 10.5194/acp-14-5639-2014, 2014.

Shang, D., Peng, J., Guo, S., Wu, Z., and Hu, M.: Secondary aerosol formation in winter haze over the Beijing-Tianjin-Hebei Region, China, Front Env. Sci. Eng., 15, 34, 10.1007/s11783-020-1326-x, 2020.

Shi, G., Xu, J., Shi, X., Liu, B., Bi, X., Xiao, Z., Chen, K., Wen, J., Dong, S., Tian, Y., Feng, Y., Yu, H., Song, S., Zhao, Q., Gao, J., and Russell, A. G.: Aerosol pH Dynamics During Haze Periods in an Urban Environment in China: Use of Detailed, Hourly, Speciated Observations to Study the Role of Ammonia Availability and Secondary Aerosol Formation and Urban Environment, J. Geophys. Res.: Atmos.

, 124, 9730-9742, https://doi.org/10.1029/2018JD029976, 2019.

Shiraiwa, M., Pfrang, C., Koop, T., and Pöschl, U.: Kinetic multi-layer model of gas-particle interactions in aerosols and clouds (KM-GAP): linking condensation, evaporation and chemical reactions of organics, oxidants and water, Atmos. Chem. Phys., 12, 2777-2794, 10.5194/acp-12-2777-2012, 2012.

Solera García, M. A., Timmis, R. J., Van Dijk, N., Whyatt, J. D., Leith, I. D., Leeson, S. R., Braban, C. F., Sheppard, L. J., Sutton, M. A., and Tang, Y. S.: Directional passive ambient air monitoring of ammonia for fugitive source attribution; a field trial with wind tunnel characteristics, Atmos. Environ., 167, 576-585, https://doi.org/10.1016/j.atmosenv.2017.07.043, 2017.

Song, C. H., Kim, C. M., Lee, Y. J., Carmichael, G. R., Lee, B. K., and Lee, D. S.: An evaluation of reaction probabilities of sulfate and nitrate precursors onto East Asian dust particles, J. Geophys. Res. Atmos., 112, D18206, https://doi.org/10.1029/2006JD008092, 2007.

Song, S., Gao, M., Xu, W., Shao, J., Shi, G., Wang, S., Wang, Y., Sun, Y., and McElroy, M. B.: Fine-particle pH for Beijing winter haze as inferred from different thermodynamic equilibrium models, Atmos. Chem. Phys., 18, 7423-7438, 10.5194/acp-18-7423-2018, 2018.

Tan, H., Cai, M., Fan, Q., Liu, L., Li, F., Chan, P., Deng, X., and Wu, D.: An analysis of aerosol liquid water content and related impact factors in Pearl River Delta, Sci. Total Environ., 579, 1822-1830, 2017.

Wang, G., Zhang, R., Gomez, M. E., Yang, L., Zamora, M. L., Hu, M., Lin, Y., Peng, J., Guo, S., and Meng, J.: Persistent sulfate formation from London Fog to Chinese haze, Proc. Natl. Acad. Sci. USA, 113, 13630-13635, 2016.

Wang, G., Chen, J., Xu, J., Yun, L., Zhang, M., Li, H., Qin, X., Deng, C., Zheng, H., Gui, H., Liu, J., and Huang, K.: Atmospheric Processing at the Sea-Land Interface Over the South China Sea: Secondary Aerosol Formation, Aerosol Acidity, and Role of Sea Salts, J. Geophys. Res.: Atmos.

, 127, e2021JD036255, https://doi.org/10.1029/2021JD036255, 2022.

Wang, H., Wang, X., Zhou, H., Ma, H., Xie, F., Zhou, X., Fan, Q., Lü, C., and He, J.: Stoichiometric characteristics and economic implications of water-soluble ions in $PM_{2.5}$ from a resource-dependent city, Environ. Res., 193, 110522, https://doi.org/10.1016/j.envres.2020.110522, 2021.

Wang, J., Li, J., Ye, J., Zhao, J., and Jacob, D. J.: Fast sulfate formation from oxidation of SO2 by NO2 and HONO observed in Beijing haze, Nat. Commun., 11, 2844, 2020.

Wang, S., Nan, J., Shi, C., Fu, Q., Gao, S., Wang, D., Cui, H., Saiz-Lopez, A., and Zhou, B.: Atmospheric ammonia and its impacts on regional air quality over the megacity of Shanghai, China, Sci. Rep., 5, 15842, 10.1038/srep15842, 2015.

Weber, R. J., Guo, H., Russell, A. G., and Nenes, A.: High aerosol acidity despite declining atmospheric sulfate concentrations over the past 15 years, Nat. Geosci., 9, 282-285, 10.1038/ngeo2665, 2016.

Wong, J. P. S., Lee, A. K. Y., and Abbatt, J. P. D.: Impacts of Sulfate Seed Acidity and Water Content on Isoprene Secondary Organic Aerosol Formation, Environ. Sci. Technol., 49, 13215-13221, 10.1021/acs.est.5b02686, 2015.

Wu, Z., Wang, Y., Tan, T., Zhu, Y., Li, M., Shang, D., Wang, H., Lu, K., Guo, S., Zeng, L., and Zhang, Y.: Aerosol Liquid Water Driven by Anthropogenic Inorganic Salts: Implying Its Key Role in Haze Formation over the North China Plain, Environ. Sci. Technol. Lett., 5, 160-166, 10.1021/acs.estlett.8b00021, 2018.

Xie, F., Zhou, X., Wang, H., Gao, J., Hao, F., He, J., and Lü, C.: Heating events drive the seasonal patterns of

volatile organic compounds in a typical semi-arid city, Sci. Total Environ., 788, 147781, https://doi.org/10.1016/j.scitotenv.2021.147781, 2021.

Xie, Y., Wang, G., Wang, X., Chen, J., Chen, Y., Tang, G., Wang, L., Ge, S., Xue, G., Wang, Y., and Gao, J.: Nitrate-dominated PM2.5 and elevation of particle pH observed in urban Beijing during the winter of 2017, Atmos. Chem. Phys., 20, 5019-5033, 10.5194/acp-20-5019-2020, 2020.

Xu, L., Duan, F., He, K., Ma, Y., Zhu, L., Zheng, Y., Huang, T., Kimoto, T., Ma, T., Li, H., Ye, S., Yang, S., Sun, Z., and Xu, B.: Characteristics of the secondary water-soluble ions in a typical autumn haze in Beijing, Environ. Pollut., 227, 296-305, https://doi.org/10.1016/j.envpol.2017.04.076, 2017.

Xue, J., Griffith, S. M., Yu, X., Lau, A. K. H., and Yu, J. Z.: Effect of nitrate and sulfate relative abundance in $PM_{2.5}$ on liquid water content explored through half-hourly observations of inorganic soluble aerosols at a polluted receptor site, Atmos. Environ., 99, 24-31, https://doi.org/10.1016/j.atmosenv.2014.09.049, 2014.

Xue, J., Yuan, Z., Griffith, S. M., Yu, X., Lau, A. K. H., and Yu, J. Z.: Sulfate Formation Enhanced by a Cocktail of High NOx, SO2, Particulate Matter, and Droplet pH during Haze-Fog Events in Megacities in China: An Observation-Based Modeling Investigation, Environ. Sci. Technol., 50, 7325-7334, 10.1021/acs.est.6b00768, 2016.

Yao, L., Fan, X., Yan, C., Kurtén, T., Daellenbach, K. R., Li, C., Wang, Y., Guo, Y., Dada, L., Rissanen, M. P., Cai, J., Tham, Y. J., Zha, Q., Zhang, S., Du, W., Yu, M., Zheng, F., Zhou, Y., Kontkanen, J., Chan, T., Shen, J., Kujansuu, J. T., Kangasluoma, J., Jiang, J., Wang, L., Worsnop, D. R., Petäjä, T., Kerminen, V.-M., Liu, Y., Chu, B., He, H., Kulmala, M., and Bianchi, F.: Unprecedented Ambient Sulfur Trioxide (SO3) Detection: Possible Formation Mechanism and Atmospheric Implications, Environ. Sci. Technol. Lett., 7, 809-818, 10.1021/acs.estlett.0c00615, 2020.

Yue, F., He, P., Chi, X., Wang, L., Yu, X., Zhang, P., and Xie, Z.: Characteristics and major influencing factors of sulfate production via heterogeneous transition-metal-catalyzed oxidation during haze evolution in China, Atmos. Pollut. Res., 11, 1351-1358, https://doi.org/10.1016/j.apr.2020.05.014, 2020.

Zhai, S., Jacob, D. J., Wang, X., Liu, Z., Wen, T., Shah, V., Li, K., Moch, J. M., Bates, K. H., Song, S., Shen, L., Zhang, Y., Luo, G., Yu, F., Sun, Y., Wang, L., Qi, M., Tao, J., Gui, K., Xu, H., Zhang, Q., Zhao, T., Wang, Y., Lee, H. C., Choi, H., and Liao, H.: Control of particulate nitrate air pollution in China, Nat. Geosci., 10.1038/s41561-021-00726-z, 2021.

Zhang, R., Wang, G., Guo, S., Zamora, M. L., Ying, Q., Lin, Y., Wang, W., Hu, M., and Wang, Y.: Formation of Urban Fine Particulate Matter, Chem. Rev., 115, 3803-3855, 10.1021/acs.chemrev.5b00067, 2015.

Zhao, Q., Nenes, A., Yu, H., Song, S., Xiao, Z., Chen, K., Shi, G., Feng, Y., and Russell, A. G.: Using High-Temporal-Resolution Ambient Data to Investigate Gas-Particle Partitioning of Ammonium over Different Seasons, Environ. Sci. Technol., 54, 9834-9843, 10.1021/acs.est.9b07302, 2020.

Zheng, B., Zhang, Q., Zhang, Y., He, K., Wang, K., Zheng, G., Duan, F., Ma, Y., and Kimoto, T.: Heterogeneous chemistry: a mechanism missing in current models to explain secondary inorganic aerosol formation during the January 2013 haze episode in North China, Atmos.Chem. Phys., 15, 2031-2049, 2015a.

Zheng, G. J., Duan, F. K., Su, H., Ma, Y. L., Cheng, Y., Zheng, B., Zhang, Q., Huang, T., Kimoto, T., Chang, D., Pöschl, U., Cheng, Y. F., and He, K. B.: Exploring the severe winter haze in Beijing: the impact of synoptic weather, regional transport and heterogeneous reactions, Atmos. Chem. Phys., 15, 2969–2983, 2015b.

Zhou, H., Lü, C., He, J., Gao, M., Zhao, B., Ren, L., Zhang, L., Fan, Q., Liu, T., He, Z., Dudagula, Zhou, B., Liu, H., and Zhang, Y.: Stoichiometry of water-soluble ions in $PM_{2.5}$: Application in source apportionment for a typical industrial city in semi-arid region, Northwest China, Atmos. Res., 204, 149-160, https://doi.org/10.1016/j.atmosres.2018.01.017, 2018.

Zhu, Y., Li, W., Lin, Q., Yuan, Q., Liu, L., Zhang, J., Zhang, Y., Shao, L., Niu, H., Yang, S., and Shi, Z.: Iron

703   solubility in fine particles associated with secondary acidic aerosols in east China, Environ. Pollut., 264,

704   114769, https://doi.org/10.1016/j.envpol.2020.114769, 2020.

705